

# RSC Advances



This is an *Accepted Manuscript*, which has been through the Royal Society of Chemistry peer review process and has been accepted for publication.

*Accepted Manuscripts* are published online shortly after acceptance, before technical editing, formatting and proof reading. Using this free service, authors can make their results available to the community, in citable form, before we publish the edited article. This *Accepted Manuscript* will be replaced by the edited, formatted and paginated article as soon as this is available.

You can find more information about *Accepted Manuscripts* in the [Information for Authors](#).

Please note that technical editing may introduce minor changes to the text and/or graphics, which may alter content. The journal's standard [Terms & Conditions](#) and the [Ethical guidelines](#) still apply. In no event shall the Royal Society of Chemistry be held responsible for any errors or omissions in this *Accepted Manuscript* or any consequences arising from the use of any information it contains.

## ARTICLE

# The luminescence properties of novel $\alpha$ -Mg<sub>2</sub>Al<sub>4</sub>Si<sub>5</sub>O<sub>18</sub>: Eu<sup>2+</sup> phosphor prepared in air

Cite this: DOI: 10.1039/x0xx00000x

Jian Chen, Yan-gai Liu\*, Haikun Liu, Dexin Yang, Hao Ding, Minghao Fang and Zhaohui Huang

Received 00th January 2012,  
Accepted 00th January 2012

DOI: 10.1039/x0xx00000x

www.rsc.org/

The  $\alpha$ -Mg<sub>2</sub>Al<sub>4</sub>Si<sub>5</sub>O<sub>18</sub>: Eu<sup>2+</sup> phosphor was firstly prepared via the conventional high temperature solid-state reaction method and the reduction of Eu<sup>3+</sup> to Eu<sup>2+</sup> in air was observed in  $\alpha$ -Mg<sub>2</sub>Al<sub>4</sub>Si<sub>5</sub>O<sub>18</sub>: Eu. The phase structure, photoluminescence (PL) properties, the PL thermal stability and the fluorescence decay curves of the samples were investigated, respectively. Emission and excitation spectra were employed to detect the presence of Eu<sup>2+</sup> ions in the compound. Under the excitation at 365 nm, the phosphor exhibited a broad-band blue emission with peak at 463 nm, which was ascribed to the 4*f*–5*d* transition of Eu<sup>2+</sup>. It was further proved that the dipole–dipole interactions resulted in the concentration quenching of Eu<sup>2+</sup> in  $\alpha$ -Mg<sub>2</sub>Al<sub>4</sub>Si<sub>5</sub>O<sub>18</sub>: xEu<sup>2+</sup> phosphors. When the temperature turned up to 150°C, the emission intensity of  $\alpha$ -Mg<sub>2</sub>Al<sub>4</sub>Si<sub>5</sub>O<sub>18</sub>: 0.12Eu<sup>2+</sup> phosphor was 59.07% of the initial value at room temperature. The activation energy  $\Delta E$  was calculated to be 0.21 eV, which proved the good thermal stability of the sample. All the properties indicated that the blue-emitting  $\alpha$ -Mg<sub>2</sub>Al<sub>4</sub>Si<sub>5</sub>O<sub>18</sub>: Eu<sup>2+</sup> phosphor has potential application in white LEDs.

## 1 Introduction

Due to their high luminous efficiency, low power consumption, and environment-friendly characteristics in comparison with traditional incandescent and currently implemented fluorescent lamps, phosphor-converted white light emitting-diodes (pc-wLEDs) have received great attention to be a next-generation light source.<sup>1</sup> Currently, commercial w-LEDs employ a blue InGaN LED chip with a yellow phosphor of Ce<sup>3+</sup>-doped yttrium aluminum garnet (YAG: Ce), and are very poor in the color rendering index (CRI) because of the color deficiency in the red region.<sup>2</sup> Consequently, w-LEDs fabricated with near ultraviolet (n-UV) LEDs chip and three primary color emissions mixed (red, green and blue) phosphors have been widely investigated.<sup>3</sup>

The luminescent properties of Eu<sup>2+</sup> ions in various matrix compounds and the reduction processes of Eu<sup>3+</sup> to Eu<sup>2+</sup> in phosphor have attracted significant attention in the past decades.<sup>4–9</sup> Normally, the photoluminescence of Eu<sup>2+</sup> in most silicates host is associated with the 4*f* → 5*d* transitions. Compared with 4*f* orbitals of Eu<sup>2+</sup>, those of 5*d* orbitals are sensitive to the changes of the crystal field strength due to its existing in the outer shell. The peak positions in the emission spectra depend strongly on the nature of the Eu<sup>2+</sup> surroundings.<sup>9</sup> Therefore Eu<sup>2+</sup> can be efficiently excited in a broad spectral range depending on the host lattices in which it is incorporated.

Generally, the reducing atmospheres, such as H<sub>2</sub>, H<sub>2</sub>/N<sub>2</sub>, or CO, is necessary to reduce Eu<sup>3+</sup> to Eu<sup>2+</sup> during the annealing process in order to prepare the optical materials activated by Eu<sup>2+</sup> ions since the raw material of the europium is Eu<sub>2</sub>O<sub>3</sub>.<sup>6,7</sup> If the reduction of Eu<sup>3+</sup> to Eu<sup>2+</sup> can be realized in air condition, it would greatly reduce the cost and increase the safety in preparing of Eu<sup>2+</sup>-activated phosphor materials. Recently, the reduction of Eu<sup>3+</sup> to Eu<sup>2+</sup> in air condition has been reported.<sup>8,10–18</sup> Since the first reported of an aliovalent substitution method to reduce trivalent rare earth ions Eu<sup>3+</sup> into divalent ions Eu<sup>2+</sup> even in air when these ions were doped in alkaline earth borate SrB<sub>4</sub>O<sub>7</sub><sup>11</sup> in 1993, there have been significant advances in LEDs. Until now, the phenomena of Eu<sup>3+</sup> reducing into Eu<sup>2+</sup> in air have been found in many systems, such as borates (SrB<sub>4</sub>O<sub>7</sub>: Eu, SrB<sub>6</sub>O<sub>10</sub>: Eu, BaB<sub>8</sub>O<sub>13</sub>: Eu and CaBPO<sub>5</sub>: Eu)<sup>8,10–13</sup>, phosphates (Ba<sub>3</sub>(PO<sub>4</sub>)<sub>2</sub>: Eu)<sup>14</sup>, sulfates (BaSO<sub>4</sub>: Eu)<sup>15</sup>, aluminates (Sr<sub>4</sub>Al<sub>14</sub>O<sub>25</sub>: Eu)<sup>16</sup>, silicates (BaMgSiO<sub>4</sub>: Eu)<sup>17</sup> and ZnO-B<sub>2</sub>O<sub>3</sub>-P<sub>2</sub>O<sub>5</sub> glasses<sup>18</sup>.

The cordierite is a magnesium/aluminium aluminosilicate with the crystallo-chemical formula Mg<sub>2</sub><sup>[6]Al<sub>3</sub><sup>[4]</sup>(Si<sub>5</sub>Al<sup>[4]</sup>O<sub>18</sub>)<sup>19</sup>, which have a complex structure with six tetrahedral units [Si/AlO<sub>4</sub>]. Binding of the tetrahedral units is ensured by the [MgO<sub>6</sub>] octahedral and [AlO<sub>4</sub>] tetrahedral. The cordierite has several polymorphic modifications. A low temperature modification ( $\beta$ -Mg<sub>2</sub>Al<sub>4</sub>Si<sub>5</sub>O<sub>18</sub>) crystallizes in the orthorhombic</sup>

system, a metastable modification ( $\mu$ - $\text{Mg}_2\text{Al}_4\text{Si}_5\text{O}_{18}$ , crystallizes from glass below  $925^\circ\text{C}$ )<sup>20</sup> crystallizes in the hexagonal and a high temperature modification ( $\alpha$ - $\text{Mg}_2\text{Al}_4\text{Si}_5\text{O}_{18}$ ) crystallizes in the hexagonal system.<sup>21</sup>

Magnesium cordierite,  $\text{Mg}_2\text{Al}_4\text{Si}_5\text{O}_{18}$ , have been used more frequently as promising ceramic material over the past several years attribute to easy preparation, chemical and thermal durability and mechanical properties resistant to corrosion at higher temperature.<sup>22-24</sup> Piriou et al.<sup>25</sup> and Thim et al.<sup>26</sup> have studied luminescent properties of magnesium cordierite ( $\text{Mg}_2\text{Al}_4\text{Si}_5\text{O}_{18}$ ) doped with  $\text{Eu}^{3+}$  ion prepared by sol-gel without any flux at  $1300^\circ\text{C}$  and  $1200^\circ\text{C}$ , respectively, and they all found the weak broad peak in the range of 420–570 nm. However, they have not further investigated about the broad peak in the range of 420–570 nm. Additionally, no further researches on the luminescence properties of  $\text{Mg}_2\text{Al}_4\text{Si}_5\text{O}_{18}$  have been reported so far. In this study, the  $\text{Mg}_2\text{Al}_4\text{Si}_5\text{O}_{18}:\text{Eu}^{2+}$  was prepared in air via using the conventional high temperature solid-state reaction method. The phase structure and luminescence properties of the blue-emitting (peak at 463nm)  $\alpha$ - $\text{Mg}_2\text{Al}_4\text{Si}_5\text{O}_{18}:\text{Eu}^{2+}$  phosphors and the mechanism of the  $\text{Eu}^{3+}$  to  $\text{Eu}^{2+}$  reduction in  $\alpha$ - $\text{Mg}_2\text{Al}_4\text{Si}_5\text{O}_{18}$  were studied in detail. These results indicate that the sample has good performance for *w*-LEDs application and it is of great significance for energy conservation.

## 2 Experimental

The  $\text{Mg}_2\text{Al}_4\text{Si}_5\text{O}_{18}:\text{Eu}^{2+}$  phosphors were prepared by conventional solid-state method with a stoichiometric quantities of  $\text{MgO}$  (A. R.),  $\text{Al}_2\text{O}_3$  (A. R.),  $\text{H}_2\text{SiO}_3$  (A. R.),  $\text{Eu}_2\text{O}_3$  (A. R.),  $\text{La}_2\text{O}_3$  (A. R.) (An excess of 8 wt% of  $\text{La}_2\text{O}_3$  was added as flux). The selected starting materials were mixed and ground homogeneously according to the given stoichiometric ratio in the agate mortar, and then some mixtures were fired at  $1300^\circ\text{C}$  in an alumina crucible for 6 hours in air. Other mixtures were sintered at the same temperature and time in the thermal carbon-reducing atmosphere (TCRA). The crystalline phases of synthesized products were examined by X-ray diffraction (XRD; D8 Advance diffractometer, Germany), using  $\text{Cu-K}\alpha 1$  radiation ( $\lambda = 1.5406 \text{ \AA}$ ) with a step of  $0.02^\circ$  ( $2\theta$ ) and a scanning rate of  $2^\circ\text{min}^{-1}$ . The emission and the excitation spectra were recorded on a Hitachi F-4600 fluorescence spectrofluorimeter.

## 3 Results and Discussion

### 3.1 Phase Structure of the Samples

Figure 1 shows the XRD patterns of  $\text{Mg}_2\text{Al}_4\text{Si}_5\text{O}_{18}$  [Fig. 1(a)],  $\text{Mg}_2\text{Al}_4\text{Si}_5\text{O}_{18}:\text{Eu}^{2+}$  [Fig. 1(b)], the standard pattern (JCPDS 84-1222) of  $\alpha$ - $\text{Mg}_2\text{Al}_4\text{Si}_5\text{O}_{18}$  and the standard pattern (JCPDS 13-0294) of  $\beta$ - $\text{Mg}_2\text{Al}_4\text{Si}_5\text{O}_{18}$ . As the Fig. 1 shows, the characteristic peak between the JCPDS card No. 13-0294 ( $\beta$ -phase) and No. 84-1222 ( $\alpha$ -phase) look like similar, while there are some difference to distinguish that the phosphor is either  $\beta$ - $\text{Mg}_2\text{Al}_4\text{Si}_5\text{O}_{18}$  or  $\alpha$ - $\text{Mg}_2\text{Al}_4\text{Si}_5\text{O}_{18}$ . It is obviously shows that the amount of characteristic peaks of  $\beta$ -phase is more than  $\alpha$ -phase

(Such as:  $23.14^\circ$  and  $37.88^\circ$ ) and XRD patterns of  $\text{Mg}_2\text{Al}_4\text{Si}_5\text{O}_{18}$  don't have any peaks on  $23.14^\circ$  and  $37.88^\circ$ . In addition, some peaks of No. 13-0294 would form the double peak phenomenon due to the distance of characteristic peaks are close [Such as: ( $26.34^\circ$ ,  $26.43^\circ$ ), ( $28.32^\circ$ ,  $28.48^\circ$ ) and ( $29.37^\circ$ ,  $29.41^\circ$ ,  $29.64^\circ$ )], while the formation of peaks of  $\text{Mg}_2\text{Al}_4\text{Si}_5\text{O}_{18}$  on  $26.19^\circ$ ,  $28.28^\circ$  and  $29.36^\circ$  are symmetrical single peaks. It indicates that the phosphors we prepared are  $\alpha$ - $\text{Mg}_2\text{Al}_4\text{Si}_5\text{O}_{18}$  (hexagonal) which crystallize in a hexagonal cell, with the space group P6/mcc, and has a hexagonal structure with the cell parameters of  $a = 9.794 \text{ \AA}$ ,  $b = 9.794 \text{ \AA}$ ,  $c = 9.339 \text{ \AA}$ ,  $V = 775.70 \text{ \AA}^3$  and  $Z = 2$ .<sup>27</sup> The miller indices for each XRD pattern are demonstrated in Fig. 1(a). It also can be seen that all the diffraction peaks of compounds are all well indexed to the standard pattern of  $\alpha$ - $\text{Mg}_2\text{Al}_4\text{Si}_5\text{O}_{18}$ , indicating that the obtained sample is single phase and the doping caused by a small amount of Eu ions did not cause the structural variation. In the  $\alpha$ - $\text{Mg}_2\text{Al}_4\text{Si}_5\text{O}_{18}:\text{Eu}^{2+}$  phosphor system, Piriou et al.<sup>25</sup> had demonstrated that the Eu ion cannot inside the structure channels at room temperature and it is assumed that  $\text{Eu}^{2+}$  ( $r = 0.117 \text{ nm}$  when coordinate number (CN) = 6) ions occupied the Mg ( $r = 0.072$  when CN = 6) sites because both the  $\text{Al}^{3+}$  ( $r = 0.039 \text{ nm}$ ) and the  $\text{Si}^{4+}$  ( $r = 0.026 \text{ nm}$ ) sites are too small to take the  $\text{Eu}^{2+}$  ions.<sup>28</sup>

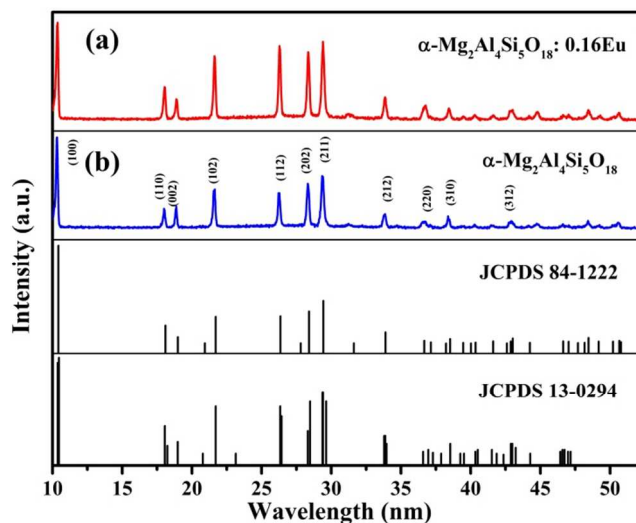


Fig. 1 XRD patterns of  $\alpha$ - $\text{Mg}_2\text{Al}_4\text{Si}_5\text{O}_{18}:\text{Eu}^{2+}$  (a),  $\alpha$ - $\text{Mg}_2\text{Al}_4\text{Si}_5\text{O}_{18}$  (b), the standard pattern (JCPDF84-1222) of  $\alpha$ - $\text{Mg}_2\text{Al}_4\text{Si}_5\text{O}_{18}$ , and the standard pattern (JCPDF13-0294) of  $\beta$ - $\text{Mg}_2\text{Al}_4\text{Si}_5\text{O}_{18}$ .

### 3.2 Luminescence properties

It is well known that the emission of  $\text{Eu}^{2+}$  ion in a solid state compound generally originated from the transition of  $4f^65d \rightarrow 4f^7$  with a broad band character. However, the emission of  $\text{Eu}^{3+}$  ion shows a narrow band character in the spectral region of 570–750 nm corresponding to  ${}^5\text{D}_0 \rightarrow {}^7\text{F}_J$  ( $J = 0-4$ ) transitions.<sup>17</sup> In consequence, the existence of  $\text{Eu}^{2+}$  ions in phosphor compounds can be detected by luminescent measurements.

Figure 2 depicts the photoluminescence (PL), photoluminescence excitation (PLE) and reflectance spectra of  $\alpha\text{-Mg}_2\text{Al}_4\text{Si}_5\text{O}_{18} : x\text{Eu}$  prepared in air. Although the precursor for europium was trivalent from  $\text{Eu}_2\text{O}_3$  and the samples were prepared by annealing at 1300 °C in air condition, it seems that the europium exists in divalent state in the compound. The PLE monitoring by 463 nm is composed of one strong absorption peak at 275 nm in the spectral range from 200 to 450 nm, which is attributed to  $4f^7(^8S_{7/2})-4f^65d$  transitions of the doped  $\text{Eu}^{2+}$  ions. PL spectrum shows that  $\alpha\text{-Mg}_2\text{Al}_4\text{Si}_5\text{O}_{18} : x\text{Eu}$  phosphor exhibits similar blue emission band peaked at 463 nm under the excitation at 365 nm, which belongs to the typical emission of  $\text{Eu}^{2+}$  ions ascribed to  $4f^65d-4f^7$  transitions.<sup>10</sup> As shown in Fig. 2, there are a part of overlap between the PL and PLE spectra of  $\alpha\text{-Mg}_2\text{Al}_4\text{Si}_5\text{O}_{18} : x\text{Eu}$ , indicates the existence of energy transfer between  $\text{Eu}^{2+}-\text{Eu}^{2+}$ .<sup>29</sup> In the reflection spectra, the  $\alpha\text{-Mg}_2\text{Al}_4\text{Si}_5\text{O}_{18}$  host material shows a high reflection in the visible range. As  $\text{Eu}^{2+}$  ions were doped into the host, a strong broad absorption appeared in the range of 200–400 nm near-UV, which assigned to the  $4f^7-4f^65d^1$  absorption of  $\text{Eu}^{2+}$  ions. The results confirm that the phosphor can match well with the emission of diffuse reflection spectrum. Additionally, we synthesized the  $\alpha\text{-Mg}_2\text{Al}_4\text{Si}_5\text{O}_{18} : \text{Eu}^{2+}$  phosphor in TCRA, and detected its PL and PLE spectra (Fig. 2) for further verification of the existence of  $\text{Eu}^{2+}$  ions in  $\alpha\text{-Mg}_2\text{Al}_4\text{Si}_5\text{O}_{18} : \text{Eu}$  prepared in air. By comparing the spectral characteristics of the PL and PLE between the air and TCRA, the shapes and positions of the PL and PLE are almost the same. However, as the inset of Fig. 2 shows, a very weak emission, which peaked at 740 nm and originated from the transition of  $^5\text{D}_0-^7\text{F}_3$  from  $\text{Eu}^{3+}$ , could be observed from the enlarged emission spectra. It can be seen clearly that most of the  $\text{Eu}^{3+}$  have been reduced to  $\text{Eu}^{2+}$  during the annealing process, while a very small amount of  $\text{Eu}^{3+}$  also exist. Hence, it indicated that the incomplete reduction of  $\text{Eu}^{3+}$  which prepared in air might be the main reason of decrement of intensity of PL from air to TCRA and it confirmed by Peng et al.<sup>16</sup> and Liu et al.<sup>30</sup> Consequently, we can conclude that the reduction of  $\text{Eu}^{3+}$  to  $\text{Eu}^{2+}$  in air took place in  $\alpha\text{-Mg}_2\text{Al}_4\text{Si}_5\text{O}_{18} : \text{Eu}$  during the preparation at high temperature.

As we can also find from the excitation spectrum, the broad-band excitation character from 200–450 nm verified that the phosphor can match well with the emission of n-UV chip. The CIE color coordinate for the  $\alpha\text{-Mg}_2\text{Al}_4\text{Si}_5\text{O}_{18}$  phosphor under 365 nm UV excitation is calculated to be (0.1674, 0.1700). These results mean that the phosphor can be used as a blue-emitting phosphor for *w*-LEDs application.

The emission ( $\lambda_{\text{ex}} = 365$  nm) spectra of  $\alpha\text{-Mg}_2\text{Al}_4\text{Si}_5\text{O}_{18} : x\text{Eu}$  ( $x = 0.02, 0.04, 0.08, 0.12, 0.16$ ) phosphors at room temperature were presented in Fig. 3. As found in Fig. 3, with an increase of Eu concentration up to 4 mol%, the intensities increase to maximum and then the emission intensity decreased with further increasing concentration, which is caused by the concentration quenching effect. From the emission spectra, the dependence of the emission intensity on the concentration of

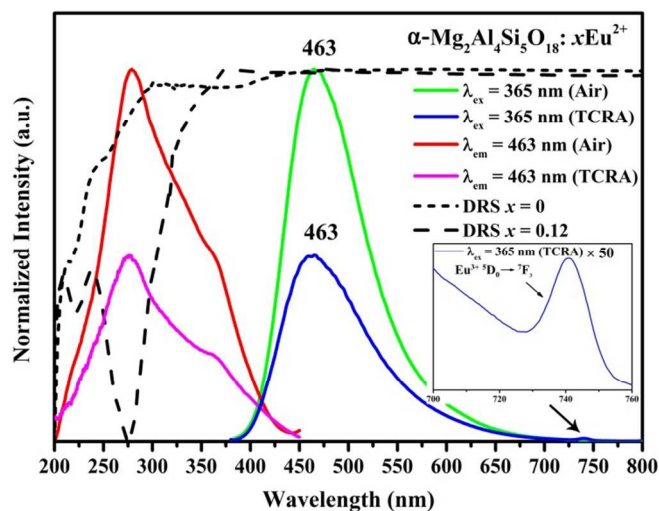


**Fig. 2** The excitation and emission spectra of  $\alpha\text{-Mg}_2\text{Al}_4\text{Si}_5\text{O}_{18} : 0.12\text{Eu}^{2+}$  ( $\lambda_{\text{em}} = 454$  nm for excitation and  $\lambda_{\text{ex}} = 365$  nm for emission) prepared in air and in TCRA; the diffuse reflection spectrum of  $\alpha\text{-Mg}_2\text{Al}_4\text{Si}_5\text{O}_{18} : x\text{Eu}^{2+}$  ( $x = 0$  and  $0.12$ ). The range of 700–760 nm of emission spectra prepared in TCRA was amplified by factor of 50. All spectra were taken at RT.

$\text{Eu}^{2+}$  is shown in the inset of Fig. 3. Thus, the optimum Eu-doping concentration is about 4 mol% for obtaining the strongest PL emission intensity. In addition, a red-shift of the peak wavelength is observed as the concentration of  $\text{Eu}^{2+}$  increases gradually, which could originate from the variations of the crystal field strength surrounding the activators.<sup>31,32</sup> When the doping concentration of  $\text{Eu}^{2+}$  increases, the inter-atomic distance between the two activators become shorter and the interaction is enhanced; as a result, the  $5d$  band of  $\text{Eu}^{2+}$  is decreased, and finally the emission wavelength is red-shifted with increasing  $\text{Eu}^{2+}$  concentration.<sup>33</sup> The mechanism of the interaction between sensitizers or between sensitizer and activator can be expressed by the following equation<sup>34,35</sup>:

$$\frac{I}{x} = K \left[ 1 + \beta(x)^\theta \right]^{-1} \quad (1)$$

where  $x$  is the activator concentration, which is not less than the critical concentration;  $I/x$  is the emission intensity ( $I$ ) per activator concentration ( $x$ );  $K$  and  $\alpha$  are constants for the same excitation condition of host crystal; and  $\theta$  is a function of multipole-multipole interaction. According to the previous reports,  $\theta = 3$  means the energy transfer among the nearest-neighbor ions and  $\theta = 6, 8$  and  $10$  corresponds to dipole–dipole (d–d), dipole–quadrupole (d–q), and quadrupole–quadrupole (q–q) interactions, respectively.<sup>36</sup> As the Fig. 4 shows, the relationship between the  $\lg(I/x)$  and  $\lg(x)$  shows a relatively linear and the slope of straight line is measured to be  $-1.8446$  which equals  $-\theta/3$ . Thus the value of  $\theta$  can be calculated to be  $5.5337$ , which is close to  $6$  that means the quenching results from dipole–dipole interactions in  $\alpha\text{-Mg}_2\text{Al}_4\text{Si}_5\text{O}_{18} : x\text{Eu}$ .

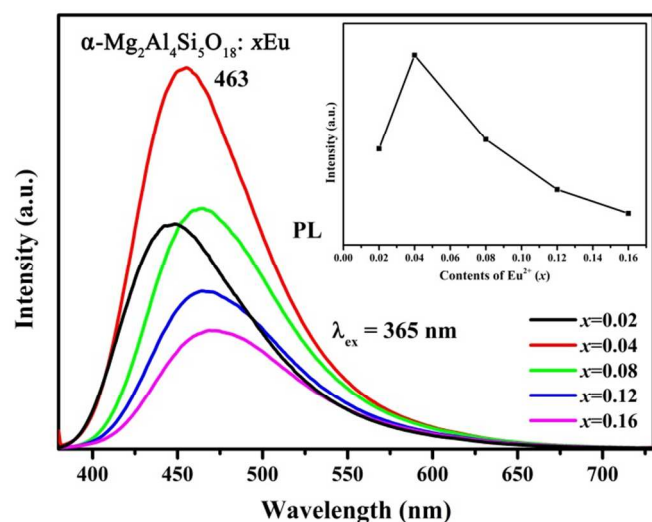


**Fig. 3** The emission spectra of  $\alpha\text{-Mg}_2\text{Al}_4\text{Si}_5\text{O}_{18}:\text{xEu}$  ( $x = 0.02, 0.04, 0.08, 0.12$  and  $0.16$ ). The inset shows the dependence of the emission intensity on the concentration of  $\text{Eu}^{2+}$ .

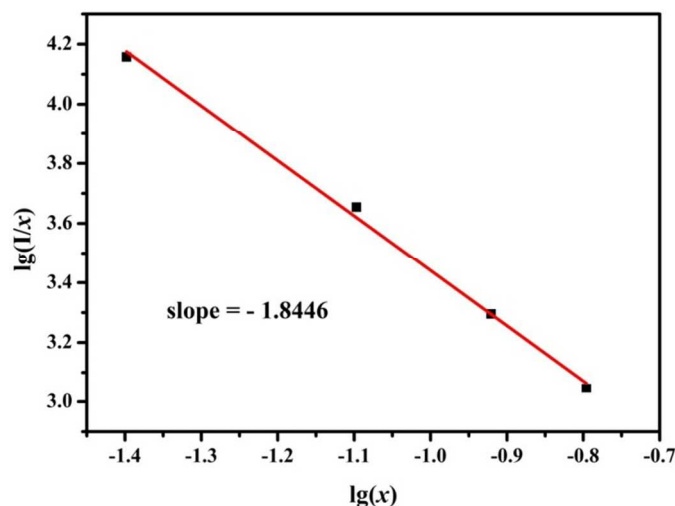


**Fig. 4** The relationship between the  $\lg(I/x)$  and  $\lg(x)$  of  $\alpha\text{-Mg}_2\text{Al}_4\text{Si}_5\text{O}_{18}:\text{xEu}^{2+}$

In general, the thermal stability of the phosphor plays an important role in solid-state lighting and has a significant influence on the light output and CRI. The temperature-dependent emission spectra under 365 nm excitation of  $\alpha\text{-Mg}_2\text{Al}_4\text{Si}_5\text{O}_{18}:\text{0.12Eu}^{2+}$  prepared in air are shown in Fig. 5. The intensity of the emission spectrum decreases with temperature increment. The emission intensities of  $\alpha\text{-Mg}_2\text{Al}_4\text{Si}_5\text{O}_{18}:\text{0.12Eu}^{2+}$  decrease to 56.95% of the initial emission intensity, which is regarded as 100%, with the increasing temperature up to 150°C. To further investigate the relationship between the photoluminescence and the temperature and to calculate the activation energy from the thermal quenching, the activation energy was calculated using the Arrhenius equation<sup>37,38</sup>:

$$I_T = \frac{I_0}{1 + c \exp\left(-\frac{\Delta E}{kT}\right)} \quad (2)$$

where  $I_0$  is the initial emission intensity of the phosphor at room temperature,  $I_T$  is the emission intensity at different temperatures,  $c$  is a constant,  $\Delta E$  is the activation energy for the thermal quenching, and  $k$  is the Boltzmann's constant ( $8.62 \times 10^{-5}$  eV). As shown in Fig. 6, the activation energy  $\Delta E$  of the thermal quenching of  $\alpha\text{-Mg}_2\text{Al}_4\text{Si}_5\text{O}_{18}:\text{0.12Eu}^{2+}$  was calculated as 0.21 eV via plotting  $\ln[(I_0/I) - 1]$  against  $1/kT$ , where a straight slope equals  $-\Delta E$ .

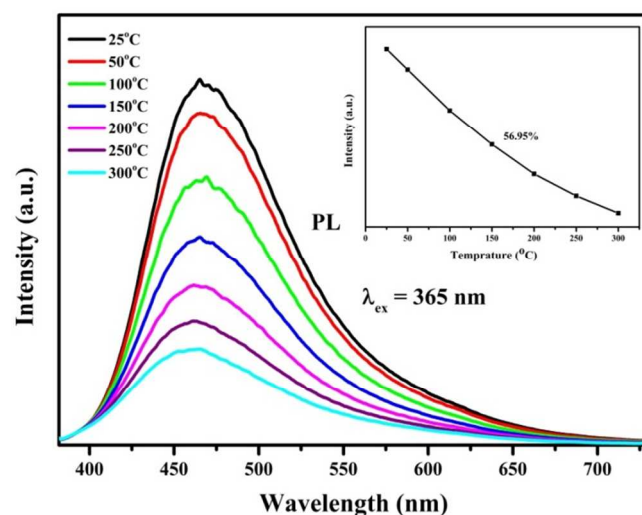


**Fig. 5** The emission spectra of  $\alpha\text{-Mg}_2\text{Al}_4\text{Si}_5\text{O}_{18}:\text{0.12Eu}^{2+}$  prepared in air at different temperatures. The inset shows the emission intensities as a function of the temperature.

Figure 7 presents the room temperature decay curves of the  $\text{Eu}^{2+}$  luminescence in  $\alpha\text{-Mg}_2\text{Al}_4\text{Si}_5\text{O}_{18}:\text{xEu}$  with different Eu contents ( $x = 0.02\text{--}0.16$ ) upon excitation at 365 nm. The entire decay curve can be well fitted to a second-order exponential decay model by the following equation<sup>39</sup>:

$$I(t) = A_1 \exp(-t/\tau_1) + A_2 \exp(-t/\tau_2) \quad (3)$$

where  $I$  is the luminescence intensity;  $A_1$  and  $A_2$  are constants;  $t$  is time; and  $\tau_1$  and  $\tau_2$  are the lifetimes for the exponential components. Further, the average lifetime constant ( $\tau^*$ ) can be calculated as

$$\tau^* = (A_1\tau_1^2 + A_2\tau_2^2)/(A_1\tau_1 + A_2\tau_2) \quad (4)$$

The obtained lifetimes monitored at 365 nm were calculated to be 613.02, 775.23, 610.01, 433.00 and 320.70 ns with Eu content = 2, 4, 8, 1.2 and 1.6 mol%, respectively. With an increase of Eu concentration up to 4 mol%, the measured lifetime  $\tau$  of  $\text{Eu}^{2+} 5d\text{--}4f$  emission increase to maximums, and then decline sharply, which is a typical sign of energy transfer, and causes concentration quenching.<sup>37</sup> The measured lifetime is also related to the total relaxation rate by:<sup>40,41</sup>

$$\frac{1}{\tau} = \frac{1}{\tau_0} + A_{nr} + P_t \quad (5)$$

where  $\tau_0$  is the radiative lifetime;  $A_{nr}$  is the nonradiative rate due to multiphonon relaxation;  $P_t$  is the energy transfer rate between  $\text{Eu}^{3+}$  ions. The distance between  $\text{Eu}^{2+}$  ions decreases with the increasing  $\text{Eu}^{2+}$  concentration. Thus, the energy transfer rate between  $\text{Eu}^{2+}$ - $\text{Eu}^{2+}$  and the probability of energy transfer to luminescent killer sites increases.<sup>42</sup> In consequence the lifetimes are shortened with increasing  $\text{Eu}^{2+}$  concentration.

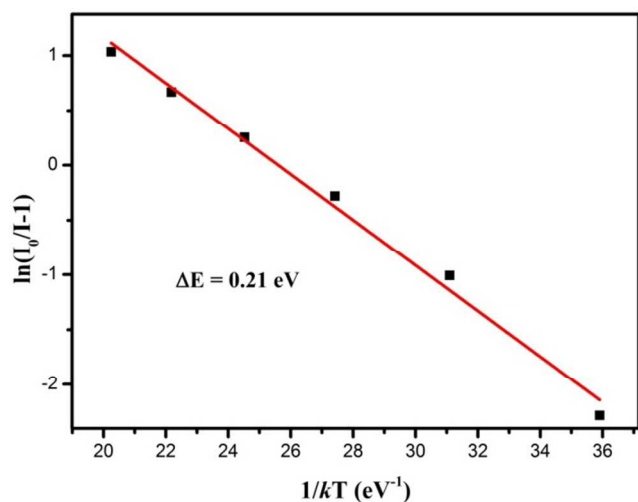


**Fig. 6** The Arrhenius fitting of the emission intensity of  $\alpha\text{-Mg}_2\text{Al}_4\text{Si}_5\text{O}_{18}: 0.12\text{Eu}^{2+}$  phosphor and the calculated activation energy ( $\Delta E$ ) for thermal quenching.

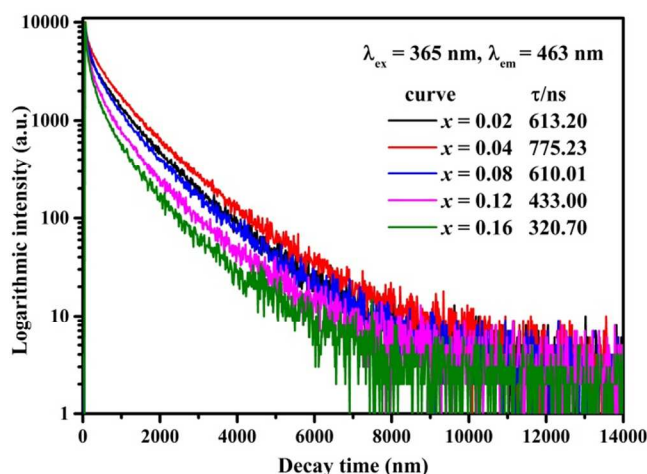
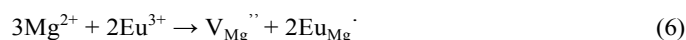


**Fig. 7** The decay curves of  $\alpha\text{-Mg}_2\text{Al}_4\text{Si}_5\text{O}_{18}: x\text{Eu}$  ( $x = 0.02 - 0.16$ ) monitored at 463 nm.

### 3.3 The mechanism of reduction $\text{Eu}^{3+} \rightarrow \text{Eu}^{2+}$ in $\alpha\text{-Mg}_2\text{Al}_4\text{Si}_5\text{O}_{18}: \text{Eu}$ prepared in air

The reduction of  $\text{Eu}^{3+}$  to  $\text{Eu}^{2+}$  in  $\alpha\text{-Mg}_2\text{Al}_4\text{Si}_5\text{O}_{18}: \text{Eu}$  in air can be explained with the charge compensation mechanism.<sup>8,16</sup> When  $\text{Eu}^{3+}$  ions were doped into  $\alpha\text{-Mg}_2\text{Al}_4\text{Si}_5\text{O}_{18}$ , the  $\text{Mg}^{2+}$  ions would be substituted non-equivalently. For the purpose of

maintaining charge balance, three  $\text{Mg}^{2+}$  ions must be replaced by two  $\text{Eu}^{3+}$  ions. Thus, each substitution of every two  $\text{Eu}^{3+}$  ion would create one vacancy defect  $V_{\text{Mg}}''$  with two negative charges, and two positive defects of  $\text{Eu}_{\text{Mg}}^{\bullet}$  in the structure. Then the vacancy of  $V_{\text{Mg}}''$  and the two  $\text{Eu}_{\text{Mg}}^{\bullet}$  defects would act as the donor of electrons and the acceptor of electrons, respectively. Consequently, under the thermal stimulation, the negative charges in vacancy defects of  $V_{\text{Mg}}''$  would be transferred into  $\text{Eu}^{3+}$  sites and reduce  $\text{Eu}^{3+}$  to  $\text{Eu}^{2+}$ . The whole process of the charge compensation mechanism could be expressed as follows:



Moreover, tetrahedral anion group composed by  $[\text{Si}/\text{AlO}_4]$  and  $[\text{AlO}_4]$  also played a role of shield for  $\text{Eu}^{2+}$  against the oxidation under the annealing process. Fig. 8 exhibits the crystal structures of hexagonal  $\alpha\text{-Mg}_2\text{Al}_4\text{Si}_5\text{O}_{18}$ .<sup>43</sup> The reduced  $\text{Eu}^{2+}$  ions substituted the  $\text{Mg}^{2+}$  ions in  $[\text{MgO}_6]$  octahedral. The  $[\text{MgO}_6]$  octahedral was surrounded by the tetrahedral framework structure which consists of corner-shared tetrahedral of  $[\text{Si}/\text{AlO}_4]$  and  $[\text{AlO}_4]$ .<sup>44</sup> For these reduced  $\text{Eu}^{2+}$  ions are located in the octahedral of 3-D network, it could effectively resist the attack of oxygen to  $\text{Eu}^{2+}$  ions and can stabilize  $\text{Eu}^{2+}$  ions.

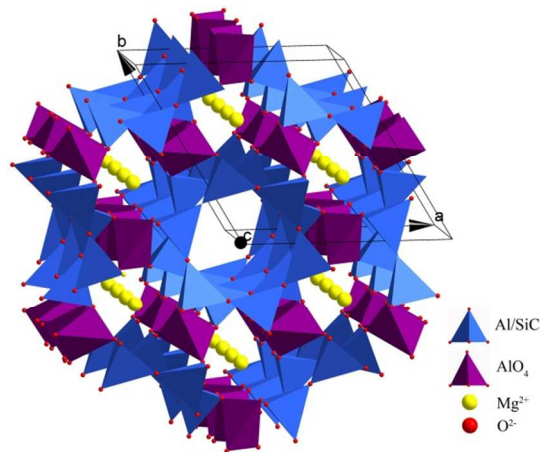


**Fig. 8** The crystal structures of  $\alpha\text{-Mg}_2\text{Al}_4\text{Si}_5\text{O}_{18}$ .

## 4 Conclusions

As a summarization, the blue-emitting  $\alpha\text{-Mg}_2\text{Al}_4\text{Si}_5\text{O}_{18}: x\text{Eu}$  phosphors were prepared in air via a high temperature solid-state reaction method. The phosphor exhibited a blue emission band peaked at 463 nm ascribed to the  $4f-5d$  transition of  $\text{Eu}^{2+}$ . As for  $\alpha\text{-Mg}_2\text{Al}_4\text{Si}_5\text{O}_{18}: x\text{Eu}^{2+}$ , the critical quenching concentration of  $\text{Eu}^{2+}$  was about 4 mol%, and the corresponding concentration quenching mechanism was verified to be the dipole-dipole interaction. The activation energy  $\Delta E$  was

calculated to be 0.21 eV, which proved the good thermal stability of the sample. The color coordinate was (0.1674, 0.1700), indicating that the  $\alpha$ -Mg<sub>2</sub>Al<sub>4</sub>Si<sub>5</sub>O<sub>18</sub>: Eu phosphor can be regarded as a blue-emitting phosphor for WL-LEDs application. The reduction of Eu<sup>3+</sup> to Eu<sup>2+</sup> in  $\alpha$ -Mg<sub>2</sub>Al<sub>4</sub>Si<sub>5</sub>O<sub>18</sub>: Eu prepared in air was explained with the charge compensation model and the structures of 3-D networks composed by [Si/AlO<sub>4</sub>] and [AlO<sub>4</sub>] tetrahedra are possible for maintaining of the reduction (Eu<sup>3+</sup>-Eu<sup>2+</sup>) when samples were prepared in air at high temperature.

### Acknowledgements

We thank the National Natural Science Foundation of China through Grant No. 51172216, the Fundamental Research Funds for the Central Universities through Grant No. 2012067 and the Program for New Century Excellent Talents in University of Ministry of Education of China through Grant No. NCET-12-0951.

### Notes and references

School of Materials Science and Technology, China University of Geosciences (Beijing), Beijing 100083, China. E-mail: liuyang@cugb.edu.cn; Tel./Fax: +86-10-82322186

- 1 H.D. Luo, J. Liu, X. Zheng, B. Xu, Y. M. Lu, L. X. Han, K. X. Ren and X. B. Yu, *J. Am. Ceram. Soc.*, 2012, **95**, 3582.
- 2 J. K. Park, M. A. Lim, C. H. Kim and H. D. Park, *Appl. Phys. Lett.*, 2003, **82**, 683.
- 3 Z. G. Xia and W.W. Wu, *Dalton.*, 2013, **42**, 12989.
- 4 G. Blasse, W.L. Wanmaker, J.W. Vrugt and A. Brill, *Philips Res. Rep.*, 1968, **189**, 23.
- 5 S. H. M. Poort, W. Janssen and G. Blasse, *J. Alloys Compd.*, 1997, **93**, 260.
- 6 C. H. Kim, I. E. Kwon, C. H. Park, Y. J. Hwang, H. S. Bae, B. Y. Yu, C. H. Pyun and G. Y. Hong, *J. Alloy. Compd.*, 2000, **311**, 33.
- 7 T. Justel, H. Bechtel, W. Mayr, and D. U. Wiechert, *J. Lumin.*, 2003, **104**, 137.
- 8 Z. W. Pei, Q. Su and J. Zhang, *J. Alloys Compd.*, 1993, **198**, 51.
- 9 S. H. M. Poort and G. Blasse, *J. Luminesc.*, 1997, **72**, 247.
- 10 Q. H. Zeng T.Z. Zhang and Z. W. Pei, *J Mater Sci Technol.*, 1999, **15**, 281.
- 11 Q. H. Zeng, Z. W. Pei, S. B. Wang and Q. Su, *J. Alloys Compd.*, 1998, **275**, 238.
- 12 H. B. Liang, Q. Su, Y. Tao, T. D. Hu and T. Liu, *J. Alloys Compd.*, 2002, **334**, 293.
- 13 Q. Su, H. B. Liang, T. D. Hu, Y. Tao, T. Liu, *J. Alloys Compd.*, 2002, **334**, 132.
- 14 I. Tale, P. Ku lis and V. Kronghauz, *J. Lumin.*, 1979, **20**, 343.
- 15 U. Madhusoodanan, M. T. Jose and A. R. Lakshmanan, *Radiat. Meas.*, 1999, **30**, 65.
- 16 M. Y. Peng, Z. W. Pei, G. Y. Hong and Q. Su, *Chem. Phys. Lett.*, 2003, **371**, 1.
- 17 M. Y. Peng, Z. W. Pei, G. Y. Hong and Q. Su, *J. Mater. Chem.*, 2003, **13**, 1202.
- 18 Z. H. Lian, J. Wang, Y.H. Lv, S.B. Wang and Q. Su, *J. Alloys Compd.*, 2007, **430**, 257.
- 19 A. N. Winchell and H. Winchell, *Academic Press*, New York, 1964.
- 20 V.L. Stolyarova, S.I. Lopatin, and O.B. Fabrichnaya, *Russ J Gen Chem.*, 2011, **10**, 2051.
- 21 The powder diffraction File, JCPDS– Joint Committee on Powder Diffraction Standards International Centre for Diffraction Data, 1997.
- 22 M. G. M. U. Ismail, H. Tsunatori, and Z. Nakai, *J. Am Ceram Soc.*, 1990, **73**, 537.
- 23 S. Kumar, K. K. Singh and P. Ramachandrarao, *J. Mater Sci Lett.*, 2000, **19**, 1263.
- 24 S. Ianoşev, I. Lazău, C. Păcurariu and A. Avramescu, *Proces Appl Ceram.*, 2008, **2**, 39.
- 25 B. Piriou, Y.F. Chen and S. Vilminot, *Eur J. Solid State Inorg Chem.*, 1998, **35**, 341.
- 26 G.P. Thim, H.F. Brito, S.A. Silva, M.A.S. Oliveira and M.C.F.C. Felinto, *J. Solid State Chem.*, 2003, **171**, 375.
- 27 P. Predecki, J. Haas, J.Faber and R. L. Hitterman, *J. Am Ceram Soc.*, 1987, **3**, 175.
- 28 Z. G. Xia, J. Zhou and Z. Y. Mao, *J. Mater. Chem.*, 2013, **1**, 5917.
- 29 Y. Guo, X. Yu, J. Liu and X. Yang, *J. Rare Earth.*, 2010, **28**, 34.
- 30 S.M. Liu, G.L. Zhao, W.R. Ruan, Z.W. Yao, T.T. Xie, J. Jin, H. Ying, J.X. Wang and Z. Nakai, *J. Am Ceram Soc.*, 2008, **91**, 2740.
- 31 T. L. Zhou, H. R. Wang, F. S. Liu, H. Zhang and Q. L. Liu, *J. Electrochem. Soc.*, 2011, **158**, 1671.
- 32 J. B. Lin and D. M. Chen, *J. Chin. Soc. Rare Earth*, 2001, **19**, 498.
- 33 C. Chartier, C. Barthou, P. Benalloul and J. M. Frigerio, *J. Lumin.*, 2005, **111**, 147.
- 34 D. L. Dexter, *J. Chem. Phys.*, 1953, **21**, 836.
- 35 G. Blasse, *Phys. Lett.*, 1968, **28**, 444.
- 36 L. Ozawa and P. M. Jaffe, *J. Electrochem. Soc.*, 1971, **118**, 1678.
- 37 R. J. Xie and N. Hirosaki, *Appl. Phys. Lett.*, 2007, **90**, 191101.
- 38 Z. G. Xia, R. S. Liu, K. W. Huang and V. Droid, *J. Mater. Chem.*, 2012, **22**, 15183.
- 39 W. J. Yang, L. Luo, T. M. Chen and N. S. Wang, *Chem. Mater.* 2005, **17**, 3883.
- 40 D. Wang and N. Kodama, *J. Solid State Chem.*, 2009, **182**, 2219.
- 41 B. Henderson and G. F. Imbusch, *Optical Spectroscopy of Inorganic Solids*, Clarendon, Oxford, 1989, p. 151.
- 42 D. Y. Wang, C. H. Huang, Y. C. Wu and T. M. Chen, *J. Mater. Chem.*, 2011, **21**, 10818.
- 43 B. Peplinski, R. Müller, K. Wenzel, R. Sojref and D. Schultze, *Mater Sci Forum.*, 2000, **321**, 150.
- 44 Z. W. Lu, L. Q. Weng, S. H. Song, P. X. Zhang, Q. Q. Hou and X. Z. Ren, *Sol-Gel Sci Technol.*, 2012, **62**, 160.